KCC Analysis of the Normal Form of Typical Bifurcations in One-Dimensional Dynamical Systems: Geometrical Invariants of Saddle-Node, Transcritical, and Pitchfork Bifurcations

Yamasaki, Kazuhito

Yajima, Takahiro

(Citation)
International Journal of Bifurcation and Chaos,27(9):1750145-1750145

(Issue Date)
2017-08

(Resource Type)
journal article

(Version)
Accepted Manuscript

International Journal of Bifurcation and Chaos

KCC analysis of the normal form of typical bifurcations in one-dimensional dynamical systems: geometrical invariants of saddle-node, transcritical, and pitchfork bifurcations

Kazuhito Yamasaki
Department of Planetology, Graduate School of Science, Kobe University, Nada, Kobe 657-8501, Japan
yk2000@kobe-u.ac.jp

Takahiro Yajima
Department of Mechanical Systems Engineering, Faculty of Engineering, Utsunomiya University, Utsunomiya, 321-8585, Japan
yajima@cc.utsunomiya-u.ac.jp

Received (to be inserted by publisher)

The Jacobi stability of the normal form of typical bifurcations in one-dimensional dynamical systems is analyzed by introducing the concept of the production process (time-like potential) to KCC theory. This KCC theory approach shows that the geometric invariants of the system characterize the non-equilibrium dynamics of the bifurcations. For example, the deviation curvature that is one of the geometric invariants shows that the well-known two hysteresis jumps in subcritical pitchfork bifurcations differ qualitatively from each other. In the non-equilibrium region, the deviation curvature in the saddle-node and the transcritical bifurcations is a function of the bifurcation parameter alone; thus, the Jacobi stability does not depend on time. However, the deviation curvature in a pitchfork bifurcation is a function of the time-like potential, so the Jacobi stability does depend on time. This time dependence can be described by the Douglas tensor, which is a useful geometric invariant to consider how the higher-order term in the bifurcation system affects the stability structure.

Keywords: Jacobi stability; KCC theory; bifurcation theory; deviation curvature; nonlinear connection; differential geometry

1. Introduction

The study of the geometric invariants of the second-order ordinary differential equation (ODE) is commonly called KCC theory (the general path-space theory of Kosambi, Cartan and Chern) (e.g., [Antonelli, & Bucataru, 2003; Sabău, 2005a; Yajima & Nagahama, 2007; Udriste & Nicola, 2007; Harko & Sabău, 2008; Balan & Neagu, 2010; Bucataru *et al.*, 2011; Neagu, 2013]). Because the dynamic system is often described by ODEs, the KCC theory has been applied to the geometric aspects of dynamic systems in various systems, such as physical (e.g., [Boehmer & Harko, 2010; Abolghasem, 2012; Harko *et al.*, 2015; Gupta & Yadav, 2016; Lake & Harko, 2016; Dănilă *et al.*, 2016]), biological (e.g., [Antonelli & Bucataru, 2001; Antonelli *et al.*, 2002; Nicola & Balan, 2004; Sabău, 2005b; Yamasaki & Yajima, 2013; Antonelli *et al.*, 2014]), and general phenomena (e.g., [Udriste & Nicola, 2009; Yajima & Yamasaki, 2016; Harko *et al.*, 2016]).

Based on one of the geometric invariants, the deviation curvature, KCC theory enables considering

Jacobi stability in bifurcations of a dynamic system (e.g., [Sabău, 2005a; Yamasaki & Yajima, 2013, 2016]). However, the subject of KCC theory is a second-order ODE, so we cannot apply KCC theory to the stability of a first-order ODE. Thus, the Jacobi stability of typical one-dimensional bifurcations described by first-order ODEs, such as the saddle-node, transcritical, and pitchfork bifurcations, has not been studied based on KCC theory. Antonelli [Antonelli, 1985, 1993], however, introduced the concept of the production process, making it possible to apply KCC theory to a first-order ODE, such as the logistic equation. Then, following Antonelli's approach, we apply KCC theory to typical one-dimensional bifurcations and consider their Jacobi stability, which is the main purpose of this study.

As an example of the production process in Antonelli's approach, we consider the logistic equation that describes the population growth:

$$\dot{n}_p = \frac{r_p}{K} n_p (K - n_p), \tag{1}$$

where n_p is the number of the population, $\dot{n}_p = dn_p/dt$, positive constants r_p and K are growth rate and carrying capacity, respectively (e.g., [Begon *et al.*, 2006]). This is a first-order ODE so we cannot apply the KCC theory to Eq. (1) itself. In Finslerian biology, Antonelli [Antonelli, 1985, 1993] introduced the concept of the production process, described by the time-like potential x_p defined as

$$n_p = a\dot{x}_p, \tag{2}$$

where $a(\neq 0)$ is a constant. Thus, Eq. (1) can be rewritten as a second-order ODE:

$$\ddot{x}_p + \frac{ar_p}{K}\dot{x}_p^2 - r_p\dot{x}_p = 0, \tag{3}$$

and we can apply KCC theory to derive the deviation curvature P^1_1 that characterizes the Jacobi stability of the system, Eq. (3) (e.g., [Antonelli, & Bucataru, 2003]):

$$P^1_1 = \frac{1}{4}r_p^2. \tag{4}$$

The definition of the deviation curvature P^i_j will be reviewed in the next section.

This approach, focusing on the deviation curvature, is useful in considering Jacobi stability; however, we need quantities to characterize the other stabilities of the system, such as the linear stability around the equilibrium points and the corresponding stability in the non-equilibrium region. For example, we consider the Malthus equation that ignores the effect of the carrying capacity K on the upper limit of the population in the logistic equation (1) (e.g., [Begon *et al.*, 2006]):

$$\dot{n}_p = r_p n_p. \tag{5}$$

By introducing a time-like potential, we can derive the deviation curvature for the Malthus equation:

$$P^1_1 = \frac{1}{4}r_p^2. \tag{6}$$

This is equal to the deviation curvature for the logistic equation (4). This means that the deviation curvature describes the essence of the growth model, but ignores the effect of the carrying capacity that is closely related to linear stability. It is known that the linear stability can be described by another geometric quantity, called the non-linear connection (e.g., [Yamasaki & Yajima, 2013, 2016]), just as the Jacobi stability can be described by the deviation curvature. In fact, the non-linear connection for the logistic equation,

$$N^1_1 = r_p\left(-\frac{1}{2} + \frac{a\dot{x}_p}{K}\right) = -\frac{r_p}{2} + \frac{r_p n_p}{K}, \tag{7}$$

is different from that of the Malthus equation:

$$N_1^1 = -\frac{r_p}{2}, \tag{8}$$

where we use (2) in the last step in (7). Note that Eqs. (7) and (8) are defined in the non-equilibrium region. When the two systems take a common equilibrium point: $n_p^* = 0$, the non-linear connection (7) is equal to (8). From these examples, this paper considers not only the deviation curvature but also the non-linear connection regarding one-dimensional bifurcations in the non-equilibrium region.

The structure of this paper is as follows. In section 2, we provide a brief review of KCC theory. In sections 3 to 6, we apply KCC theory to typical examples of one-dimensional bifurcation phenomena: saddle-node (section 3), transcritical (section 4), supercritical pitchfork (section 5), and subcritical pitchfork (section 6). The ODE analyzed in this paper is in the normal form [Wiggins, 2003; Strogatz, 2014]. That is, for the function $n = n(t)$ and the bifurcation parameter r, the ODE with a saddle-node bifurcation is $\dot{n} = r+n^2$; a transcritical bifurcation is $\dot{n} = rn-n^2$; a supercritical pitchfork bifurcation is $\dot{n} = rn-n^3$; and a subcritical pitchfork bifurcation is $\dot{n} = rn+n^3-n^5$. In section 7, we discuss the results from the viewpoint of time-dependence of the invariant quantities in KCC theory. Section 8 is devoted to our conclusions.

2. Basic theory

2.1. *A brief review of KCC theory*

Let M be a real, smooth n-dimensional manifold, and (TM, π, M) be its tangent bundle, where $\pi : TM \to M$ is a projection from the total space TM to the base manifold M. A point $x \in M$ has local coordinates (x^i), where $i = 1, \ldots, n$. The local chart of a point in TM is indicated by $(x^i, \dot{x}^i)$, where t is time (regarded as an absolute invariant) and $\dot{x}^i = dx/dt$.

Let us consider the path equation

$$\ddot{x}^i + g^i(x, \dot{x}) = 0, \tag{9}$$

where $g^i(x, \dot{x})$ is a smooth function. By adding a small perturbation to the trajectory of (9), we can obtain a variational equation. According to KCC theory (e.g., [Antonelli, & Bucataru, 2003]), the covariant form of the variational equation is given by

$$\frac{D^2 u^i}{Dt^2} = P^i_j u^j, \tag{10}$$

where $D(\cdots)/Dt$ is a covariant differential. P^i_j is the geometric object called the deviation curvature tensor. This is defined by the following relation:

$$P^i_j = -\frac{\partial g^i}{\partial x^j} + \frac{\partial N^i_j}{\partial x^k}\dot{x}^k - G^i_{jk}g^k + N^i_k N^k_j, \tag{11}$$

where N^i_j is a coefficient of the non-linear connection:

$$N^i_j = \frac{1}{2}\frac{\partial g^i}{\partial \dot{x}^j}, \tag{12}$$

and G^i_{jk} is a Finsler (Berwald) connection:

$$G^i_{jk} = \frac{\partial N^i_j}{\partial \dot{x}^k}. \tag{13}$$

The Jacobi stability can be interpreted as representing the robustness of a trajectory of the system, with respect to small perturbations of the whole trajectory [Lake & Harko, 2016; Sabău, 2005a]. According

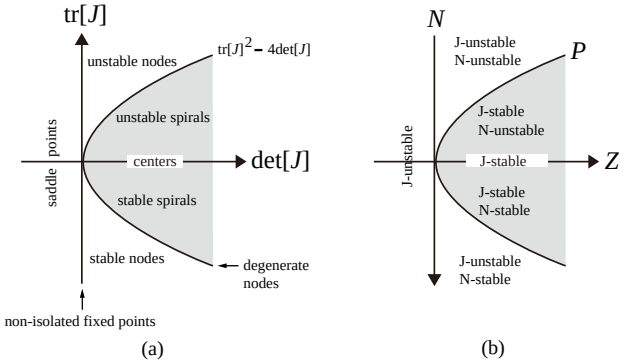

Fig. 1. Type and stability of the equilibrium points (modified from [Yamasaki & Yajima, 2013]). (a) The well-known diagram is expressed in terms of Jacobian J of the linearized system around the equilibrium points. (b) The corresponding diagram expressed in terms of the geometrical quantities from KCC theory. Note that the N-axis is reversed. From [Yamasaki & Yajima, 2013], $N = -(1/2)\mathrm{tr}[J]$, $Z = \det[J]$ and $P = N^2 - Z$.

to previous studies [Antonelli, & Bucataru, 2003; Sabău, 2005a,b], the trajectories of the one-dimensional system are Jacobi stable when $P_1^1 < 0$, and Jacobi unstable when $P_1^1 \geq 0$. In this paper, we call the system J-stable when $P_1^1 < 0$ and J-unstable when $P_1^1 \geq 0$. Around the equilibrium points, J-stable and J-unstable correspond to spiral and node, respectively (e.g., [Sabău, 2005b; Yamasaki & Yajima, 2013, 2016]). Moreover, in this paper, we call the system N-stable when $N_1^1 > 0$, N-unstable when $N_1^1 < 0$, and N-neutral when $N_1^1 = 0$. Around the equilibrium points, N-stable, N-unstable, and N-neutral correspond to linear stable, linear unstable, and neutral, respectively [Yamasaki & Yajima, 2013, 2016]. The relationship between the stability type of the bifurcation theory and the geometric terms of KCC theory is summarized in Fig.1 [Yamasaki & Yajima, 2013].

For example, we consider the logistic system given by the second-order ODE (3). From (11), (12), and (13), the geometric quantities of the logistic system are given by (4) and (7). Around the equilibrium points, $n_p^* = 0$ and $n_p^* = K$, the deviation curvature (4) remains the same and positive, and only the non-linear connection (7) changes: $N_1^1 = -r/2 < 0$ for $n_p^* = 0$ and $N_1^1 = r/2 > 0$ for $n_p^* = K$. From Fig.1, this means that $n_p^* = 0$ is the unstable node, and $n_p^* = K$ is the stable node. Next, we consider the non-equilibrium region of the logistic system. The deviation curvature (4) shows that the logistic system is J-unstable ($P_1^1 > 0$), independent of the number of the population. The non-linear connection (7) shows that the system becomes N-unstable ($N_1^1 < 0$) from N-stable ($N_1^1 > 0$) at the critical point $n_p = K/2$. Non-equilibrium dynamics near the critical point $n_p = K/2$ are not trivial from the viewpoint of local analysis around the equilibrium points.

2.2. *Deviation curvature for production process*

Let us consider the first-order ODE for n:

$$\dot{n}^i + f(n) = 0, \tag{14}$$

where $f(n)$ is a polynomial function for n^i such as $-rn_p + (r/K)n_p^2$ in Eq. (1). We define the time-like potential $x^i = x^i(t)$ as

$$n^i = a\dot{x}^i, \tag{15}$$

where $a(\neq 0)$ is a constant. Then, we have the second-order ODE for x^i:

$$\ddot{x}^i + g^i(\dot{x}) = 0, \tag{16}$$

where g^i is a polynomial function for only $\dot{x}$ such as $(ar/K)\dot{x}_p^2 - r\dot{x}_p$ in the case of Eq. (3). This means that $\partial g^i/\partial x^j = 0$ and $\partial N_j^i/\partial x^k = 0$. Then, the deviation curvature (11) for the production process is simplified:

$$P^i_j = -G^i_{jk}g^k + N^i_k N^k_j. \tag{17}$$

In the following analysis, we use (17) with (12) and (13). Because we consider the one-dimensional case in this paper, we set $n^1 = n$, $x^1 = x$, $g^1 = g$, $G^1_{11} = G$, $N^1_1 = N$, and $P^1_{11} = P$ for simplicity.

3. Saddle-node bifurcation

3.1. *Brief summary*

The normal form of the ODE with a saddle-node bifurcation is

$$\dot{n} = r + n^2, \tag{18}$$

where r is the bifurcation parameter. From $\dot{n} = 0$, we have the equilibrium points $n^*_\pm = \pm\sqrt{-r}$. If $r < 0$, there are two equilibrium points: a stable one n^*_-, and an unstable one n^*_+. At $r = 0$, there is one equilibrium point: $n^*_\pm = 0$. If $r > 0$, there is no equilibrium point. That is, two equilibrium points move towards each other ($r < 0$), collide ($r = 0$), and mutually annihilate ($r > 0$), the so-called saddle-node bifurcation.

3.2. *Dynamics of production process in non-equilibrium region*

We consider the saddle-node bifurcation from the viewpoint of KCC theory. Substitution of the time-like potential, defined by (15), into the normal form (18) leads to

$$\ddot{x} + g = 0, \tag{19}$$

with

$$g = -\frac{r}{a} - a\dot{x}^2. \tag{20}$$

From (12), (13) and (17), we can obtain the differential geometric quantities that characterize the saddle-node bifurcation in the non-equilibrium region:

$$N = -a\dot{x} = -n, \tag{21}$$

$$G = -a, \tag{22}$$

$$P = -r. \tag{23}$$

From KCC theory, these geometric quantities are related to the stability of the production process in the saddle-node bifurcation. As mentioned in the previous section, N-stability is determined by the sign of the non-linear connection N, and J-stability is determined by the sign of the deviation curvature P (e.g., [Yamasaki & Yajima, 2013]). Thus, from (21) and (23), we have four kinds of dynamics, as follows:

(1) $r \leq 0$
   (a) For $n > 0$, the system is N-unstable ($N < 0$) and J-unstable ($P \geq 0$).
   (b) For $n < 0$, the system is N-stable ($N > 0$) and J-unstable.

(2) $r > 0$
   (a) For $n > 0$, the system is N-unstable and J-stable ($P < 0$).
   (b) For $n < 0$, the system is N-stable and J-stable.

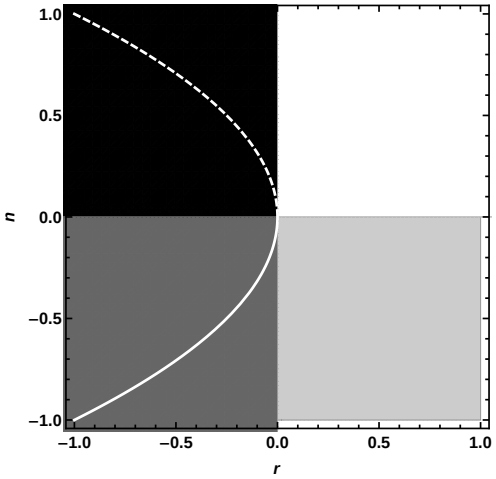

Fig. 2. N-stability and J-stability for a saddle-node bifurcation. The white (black) region shows N-unstable and J-stable (unstable) areas. The light (dark) gray region shows N-stable and J-stable (unstable) areas. The white line indicates the linear stable equilibrium point, and the dotted line indicates the linear unstable one.

These results are illustrated in Fig.2. White and black regions show the N-unstable regions, but the former is J-stable and the latter is J-unstable. Light and dark gray regions show the N-stable regions, but the former is J-stable and the latter is J-unstable. The white line indicates the equilibrium points $n^*_\pm = \pm\sqrt{-r}$. From section 3.1, the normal white line is linear stable, and the dotted white line is linear unstable. The normal line and the dotted line are included in N-stable region and N-unstable region, respectively, because around the equilibrium points, N-stable and N-unstable correspond to linear stable and linear unstable, respectively (e.g., [Yamasaki & Yajima, 2013]). Around the equilibrium points, J-stable and J-unstable correspond to spiral and node, respectively (e.g., [Yamasaki & Yajima, 2013]).

Figure 2 shows that we can see the dynamics far from the white line (the equilibrium points). This is one of the useful points of applying KCC theory to a stability analysis. Because two equilibrium points annihilate, the region $r > 0$ has no equilibrium points. Figure 2 shows that this region is not simple but consists of two different stable regions: the white and the light gray regions. This means that by adding a small perturbation to the system in the non-equilibrium region, the N-stability differs. However, the J-stability of the region $r > 0$ is the same, i.e., J-stable, so the non-equilibrium dynamics of the production process in the region $r > 0$ includes spiral-like behavior, even though the field itself obeys the saddle-node bifurcations around the equilibrium points.

3.3. *Dynamics of production process around equilibrium points*

Let us consider the dynamics of the production process around the equilibrium points: $n = n^*_\pm = \pm\sqrt{-r}$. In this case, from (21), only the non-linear connection changes:

$$N = -n^*_\pm = \mp\sqrt{-r}. \tag{24}$$

As mentioned above, around the equilibrium points, J-stability corresponds to node or spiral, and N-stability corresponds to linear stability (Fig.1). If $r < 0$, we have a linear stable point $N = \sqrt{-r} > 0$ and a linear unstable point $N = -\sqrt{-r} < 0$. From (23), we have J-unstable ($P > 0$), so the equilibrium points are node (Fig.1). By combining these results, when $r < 0$, there are two equilibrium points: a stable node point and an unstable node point. At $r = 0$, the equilibrium points collide and mutually annihilate for $r > 0$. This means that the production process also shows the saddle-node bifurcation around the equilibrium points.

4. Transcritical bifurcation

4.1. *Brief summary*

The normal form of an ODE with a transcritical bifurcation is

$$\dot{n} = rn - n^2. \tag{25}$$

From $\dot{n} = 0$, we have the equilibrium points: $n_0^* = 0$ and $n_r^* = r$. If $r < 0$, there are two equilibrium points: an unstable one n_r^*, and a stable one n_0^*. At $r = 0$, there is one equilibrium point: $n_0^* = n_r^* = 0$. If $r > 0$, there are two equilibrium points: an unstable one n_0^* and a stable one n_r^*. That is, the equilibrium point changes its stability when r is varied, the so-called transcritical bifurcation.

4.2. *Dynamics of production process in non-equilibrium region*

Substitution of (15): $n = a\dot{x}$ into (25) leads to

$$\ddot{x} + g = 0, \tag{26}$$

with

$$g = -r\dot{x} + a\dot{x}^2. \tag{27}$$

From (12), (13), and (17), we can obtain the differential geometric quantities that characterize the transcritical bifurcation in the non-equilibrium region:

$$N = -\frac{1}{2}r + a\dot{x} = -\frac{1}{2}r + n, \tag{28}$$

$$G = a, \tag{29}$$

$$P = \frac{r^2}{4}. \tag{30}$$

Thus, from the sign of the non-linear connection and the deviation curvature, the system shows the following dynamics. Because the Jacobi stability is always unstable from Eq. (30), there are two kinds of dynamics in the non-equilibrium region:

(1) For $n > r/2$, the system is N-stable and J-unstable.
(2) For $n < r/2$, the system is N-unstable and J-unstable.

These results are illustrated in Fig.3. In the case of the saddle-node bifurcation, the non-linear connection and the deviation curvature correspond to the field n and the bifurcation parameter r, respectively (Eqs. (21) and (23)), so the geometric pattern of the stability shows four simple quadrants (Fig.2). However, as we will see in the following bifurcations (sections 5 and 6), including the transcritical case, the geometric quantities will be a function of both of n and r, so the stability in the non-equilibrium region will show various geometric patterns.

From Fig.3, the relative difference of the gradient of the straight lines is related to the stability structure. That is, the gradient of an equilibrium line $n = r$ is larger than the gradient of a boundary line between the black region and the dark gray region: $n = r/2$. Therefore, when the bifurcation parameter r increases, the equilibrium line can pass the boundary line, and its unstable state becomes stable. On the other hand, an another equilibrium line $n = 0$ is passed by the boundary line, so its stable state becomes unstable.

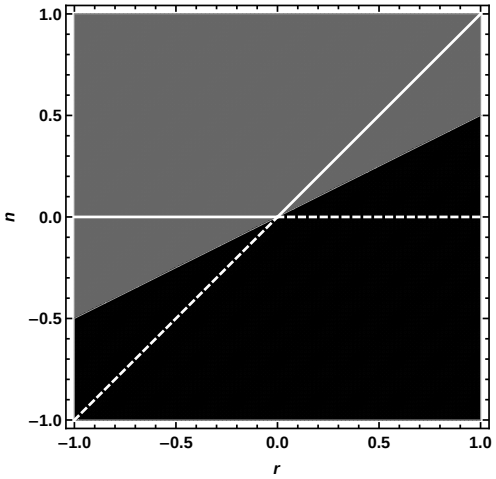

Fig. 3. N-stability and J-stability for a transcritical bifurcation. The black region shows N-unstable and J-unstable areas. The dark gray region shows N-stable and J-unstable areas. The white line indicates the linear stable equilibrium point, and the dotted line indicates the linear unstable one.

4.3. *Dynamics of production process around equilibrium points*

Let us consider the dynamics of the production process around the equilibrium points: $n_0^* = 0$ and $n_r^* = r$. In this case, from (28), only the non-linear connection changes:

$$N = \begin{cases} -\frac{1}{2}r, & n_0^* = 0, \\ \frac{1}{2}r, & n_r^* = r. \end{cases} \tag{31}$$

Because the deviation curvature is always positive (30), the dynamics around the equilibrium points are always node type (Fig.1). From the sign of the non-linear connection, when $r < 0$, there is an unstable node point, $n_r^* = r$, and a stable node point, $n_0^* = 0$. When $r > 0$, there is an unstable node point, $n_0^* = 0$, and a stable node point, $n_r^* = r$. That is, the equilibrium point changes its stability when r is varied. This means that the production process also shows a transcritical bifurcation around the equilibrium points.

5. Supercritical pitchfork bifurcation

5.1. *Brief summary*

The normal form of the ODE with a supercritical pitchfork bifurcation is

$$\dot{n} = rn - n^3. \tag{32}$$

From $\dot{n} = 0$, we have the equilibrium points $n_0^* = 0$ and $n_\pm^* = \pm\sqrt{r}$. If $r \leq 0$, there is one stable equilibrium point: n_0^*. If $r > 0$, there are three equilibrium points: an unstable one n_0^* and stable ones $n_\pm^*$. That is, when r is varied, two new equilibrium points appear on either side of the origin, the so-called supercritical pitchfork bifurcation.

5.2. *Dynamics of production process in non-equilibrium region*

Substitution of (15): $n = a\dot{x}$ into (32) leads to

$$\ddot{x} + g = 0, \tag{33}$$

with

$$g = -r\dot{x} + a^2\dot{x}^3. \tag{34}$$

From (12), (13), and (17), we can obtain the differential geometric quantities that characterize the supercritical pitchfork bifurcation in the non-equilibrium region:

$$N = \frac{1}{2}(-r + 3a^2\dot{x}^2) = \frac{1}{2}(-r + 3n^2), \tag{35}$$

$$G = 3a^2\dot{x} = 3an, \tag{36}$$

$$P = \frac{1}{4}(r^2 + 6ra^2\dot{x}^2 - 3a^4\dot{x}^4) = \frac{1}{4}(r^2 + 6rn^2 - 3n^4). \tag{37}$$

First, we consider N-stability in the non-equilibrium region. From (35), we have $N > 0$ for $3n^2 > r$, and $N < 0$ for $3n^2 < r$. Because n is a real number, the system is always N-stable ($N > 0$) for $r < 0$. That is, N-stability depends on r for $r > 0$. From $\sqrt{r/3} \approx 0.58\sqrt{r}$, we have

(1) $r > 0$
   (a) N-stable for $n < -0.58\sqrt{r}$ and $n > 0.58\sqrt{r}$.
   (b) N-unstable for $-0.58\sqrt{r} < n < 0.58\sqrt{r}$.

(2) $r < 0$
   (a) N-stable for any n.

Next, we consider J-stability based on (37). The equation for n: $r^2 + 6rn^2 - 3n^4 = 0$ has four solutions: $n = \pm\sqrt{r - 2r/\sqrt{3}} \approx \pm 0.39\sqrt{-r}$ and $n = \pm\sqrt{r + 2r/\sqrt{3}} \approx \pm 1.47\sqrt{r}$. Therefore, the property of J-stability depends on the sign of r. Specifically, we have

(1) $r < 0$
   (a) J-stable for $n < -0.39\sqrt{-r}$ and $n > 0.39\sqrt{-r}$.
   (b) J-unstable for $-0.39\sqrt{-r} \le n \le 0.39\sqrt{-r}$.

(2) $r > 0$
   (a) J-stable for $n < -1.47\sqrt{r}$ and $n > 1.47\sqrt{r}$.
   (b) J-unstable for $-1.47\sqrt{r} \le n \le 1.47\sqrt{r}$.

From the combination of N-stability and J-stability, we have the following dynamics in the non-equilibrium region:

(1) $r > 0$
   (a) N-stable and J-stable for $n < -1.47\sqrt{r}$ and $n > 1.47\sqrt{r}$.
   (b) N-unstable and J-unstable for $-0.58\sqrt{r} < n < 0.58\sqrt{r}$.
   (c) N-stable and J-unstable for $-1.47\sqrt{r} \le n < -0.58\sqrt{r}$ and $0.58\sqrt{r} < n \le 1.47\sqrt{r}$.

(2) $r < 0$
   (a) N-stable and J-stable for $n < -0.39\sqrt{-r}$ and $n > 0.39\sqrt{-r}$.
   (b) N-stable and J-unstable for $-0.39\sqrt{-r} \le n \le 0.39\sqrt{-r}$.

These results are summarized in Fig.4. In the previous sections, the deviation curvature did not depend on time, i.e., P was a function of only the bifurcation parameter r, such as Eqs. (23) and (30). However, Eq. (37) shows that the deviation curvature depends on time: i.e., P is a function of r and n. Therefore, the geometric pattern in the r-n diagram (Fig.4) becomes relatively complex, compared with those in Figs.2 and 3. Even if the geometrical pattern becomes complex, the white line (the equilibrium points) is always included in the dark gray and black regions (J-unstable region). That is, the non-equilibrium region of the

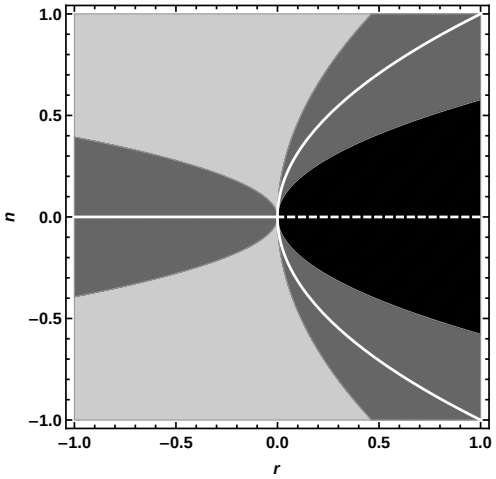

Fig. 4. N-stability and J-stability for a supercritical pitchfork bifurcation. The black region shows N-unstable and J-unstable areas. The light (dark) gray region shows N-stable and J-stable (unstable). The white line indicates the linear stable equilibrium point, and the dotted line indicates the linear unstable one.

dynamics can include the J-stable region. This J-stable region is always N-stable, because there is no white region.

5.3. *Dynamics of production process around equilibrium points*

Next, we consider the dynamics of the production process around the equilibrium points: $n_0^* = 0$ and $n_\pm^* = \pm\sqrt{r}$. In this case, from Eqs. (35) and (37), the non-linear connection and the deviation curvature become

$$N = \begin{cases} -\frac{1}{2}r, & n_0^* = 0, \\ r, & n_\pm^* = \pm\sqrt{r}. \end{cases} \tag{38}$$

$$P = \begin{cases} \frac{1}{4}r^2, & n_0^* = 0, \\ r^2, & n_\pm^* = \pm\sqrt{r}. \end{cases} \tag{39}$$

Because the equilibrium points are a real number, when $r \leq 0$, there is one equilibrium point: $n_0^* = 0$. This is a stable node point from $N \geq 0$ and $P \geq 0$ (Fig.1). In a similar fashion, when $r > 0$ there are two stable node points, $n_\pm^* = \pm\sqrt{r}$, and one unstable node point, $n_0^* = 0$. Therefore, the production process also shows a supercritical pitchfork bifurcation when r is varied.

6. Subcritical pitchfork bifurcation

6.1. *Brief summary*

The canonical example of a system with a subcritical pitchfork bifurcation is given by

$$\dot{n} = rn + n^3 - n^5. \tag{40}$$

When we ignore the higher-order term n^5, the system is accompanied by explosive instability. In real physical systems, such an explosive instability is usually opposed by the stabilizing influence of higher-order terms [Strogatz, 2014], so we add the term n^5 in this section.

From $\dot{n} = 0$, we have five equilibrium points:

$$n_0^* = 0, \tag{41}$$

$$n^*_{a\pm} = \pm\frac{\sqrt{1-\sqrt{1+4r}}}{\sqrt{2}}, \tag{42}$$

$$n^*_{b\pm} = \pm\frac{\sqrt{1+\sqrt{1+4r}}}{\sqrt{2}}. \tag{43}$$

When r is varied, this system also shows the pitchfork bifurcation, as in the previous section. That is, one stable point n^*_0 for $r < -1/4$, three stable points n^*_0 and $n^*_{b\pm}$, and two unstable points $n^*_{a\pm}$ for $-1/4 \le r \le 0$, and two stable points $n^*_{b\pm}$ and one unstable point n^*_0 for $r > 0$.

The new feature in the subcritical one is that unstable branches turn around in the n-r diagram when $r = 0$. It is known that the feature is accompanied by hysteresis: a lack of reversibility as a parameter is varied. The concept of the hysteresis has been of scientific and practical interest (e.g., [Borresen & Lynch, 2002; Burguete & De La Torre, 2009; Ramos *et al.*, 2017]).

6.2. *Dynamics of production process in non-equilibrium region*

Substitution of (15): $n = a\dot{x}$ into (40) leads to

$$\ddot{x} + g = 0, \tag{44}$$

with

$$g = -r\dot{x} - a^2\dot{x}^3 + a^4\dot{x}^5. \tag{45}$$

From (12), (13), and (17), we can obtain the differential geometric quantities that characterize the subcritical pitchfork bifurcation in the non-equilibrium region:

$$N = \frac{1}{2}(-r - 3a^2\dot{x}^2 + 5a^4\dot{x}^4) = \frac{1}{2}(-r - 3n^2 + 5n^4), \tag{46}$$

$$G = a^2\dot{x}(-3 + 10a^2\dot{x}^2) = an(-3 + 10n^2), \tag{47}$$

$$\begin{aligned} P &= \frac{1}{4}\{r^2 - 3(a\dot{x})^4 + 22(a\dot{x})^6 - 15(a\dot{x})^8 + 6r(a\dot{x})^2(-1 + 5(a\dot{x})^2)\} \\ &= \frac{1}{4}\{r^2 - 3n^4 + 22n^6 - 15n^8 + 6rn^2(-1 + 5n^2)\}. \end{aligned} \tag{48}$$

First, we consider N-stability in the non-equilibrium region. When $N = 0$ in Eq. (46), we have four solutions:

$$n_{a\pm} = \pm\frac{\sqrt{3-\sqrt{9+20r}}}{\sqrt{10}}, \tag{49}$$

$$n_{b\pm} = \pm\frac{\sqrt{3+\sqrt{9+20r}}}{\sqrt{10}}. \tag{50}$$

Based on (49) and (50), N-stability of the subcritical pitch- fork bifurcation can be considered as follows.

(1) $r < -9/20$

(a) N-stable for any n.

(2) $-9/20 < r < 0$
  (a) N-stable for $n < n_{b-}$, $n_{a-} < n < n_{a+}$ and $n > n_{b+}$.
  (b) N-unstable for $n_{b-} < n < n_{a-}$ and $n_{a+} < n < n_{b+}$.

(3) $r > 0$
  (a) N-stable for $n < n_{b-}$ and $n > n_{b+}$.
  (b) N-unstable for $n_{b-} < n < n_{b+}$.

Next, we consider J-stability. When $P = 0$ in Eq. (48), we have eight solutions $n_{i\pm}$ $(i = 1, 2, 3, 4)$:

$$n_{1\pm} = \pm\sqrt{A_- - B_-}, \quad n_{2\pm} = \pm\sqrt{A_- + B_-}, \quad n_{3\pm} = \pm\sqrt{A_+ - B_+}, \quad n_{4\pm} = \pm\sqrt{A_+ + B_+}, \tag{51}$$

with

$$A_\pm = \frac{11}{30} \pm \frac{1}{2}\sqrt{\omega + \gamma}, \quad B_\pm = \frac{1}{2}\sqrt{-\omega \pm \frac{\delta}{4\sqrt{\omega + \gamma}} + 2\gamma}, \tag{52}$$

$$\omega = \frac{\alpha}{15} + \frac{\beta}{15\alpha}, \tag{53}$$

$$\alpha = \left\{1 - 4r(-9 + 68r + 400r^2) + 8\sqrt{r^2(1 + 4r)^2(-19 + 200r(-3 + 10r))}\right\}^{1/3}, \tag{54}$$

$$\beta = (1 + 4r)(1 + 20r), \quad \gamma = \frac{91}{225} + \frac{4}{3}r, \quad \delta = \frac{32}{3375}(209 + 900r). \tag{55}$$

From the sign of the deviation curvature, J-stability of the subcritical pitchfork bifurcation can be considered as follows.

(1) $r < -0.25$
  (a) J-stable for $n < n_{2-}$ and $n > n_{2+}$.
  (b) J-unstable for $n_{2-} \le n \le n_{2+}$.

(2) $-0.25 < r < -0.029$
  (a) J-stable for $n < n_{4-}$ and $n > n_{4+}$.
  (b) J-unstable for $n_{4-} \le n \le n_{4+}$.

(3) $-0.029 < r < 0.33$
  (a) J-stable for $n < n_{4-}$, $n > n_{4+}$, $n_{3-} < n < n_{2-}$ and $n_{2+} < n < n_{3+}$.
  (b) J-unstable for $n_{4-} \le n \le n_{3-}$ and $n_{3+} \le n \le n_{4+}$.

(4) $r > 0.33$
  (a) J-stable for $n < n_{4-}$ and $n > n_{4+}$.
  (b) J-unstable for $n_{4-} \le n \le n_{4+}$.

The combination of N-stability and J-stability is summarized in Fig.5. Compared with the supercritical one (Fig.4), the subcritical one has the white region in which the system is N-unstable and J-stable. The existence of the white region makes the jump process in the hysteresis phenomena more complex.

Suppose we decrease the parameter r along the large-amplitude of the stable equilibrium point (43): $n^*_{b\pm} = \pm\sqrt{1 + \sqrt{1 + 4r}}/\sqrt{2}$, and see the jump from it to another stable equilibrium point $n^*_0 = 0$ at $r = -1/4$ through the non-equilibrium region. From Fig.6, this non-equilibrium region is J-unstable (the black and the dark gray regions). However, suppose we increase r along the stable equilibrium point n^*_0, and see the jump to the large-amplitude $n^*_{b\pm}$ at $r = 0$. Because the white region exists, this jump process includes not only a J-unstable region but also a J-stable region (Fig.6). Thus, it is found that the two

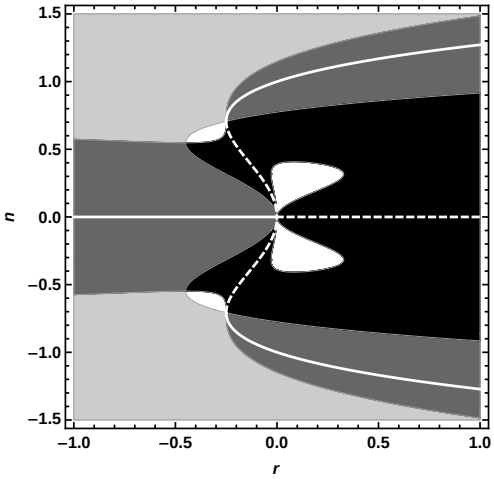

Fig. 5. N-stability and J-stability for a subcritical pitchfork bifurcation. The white (black) region shows N-unstable and J-stable (unstable) areas. The light (dark) gray region shows N-stable and J-stable (unstable) areas. The white line indicates the linear stable equilibrium point, and the dotted line indicates the linear unstable one.

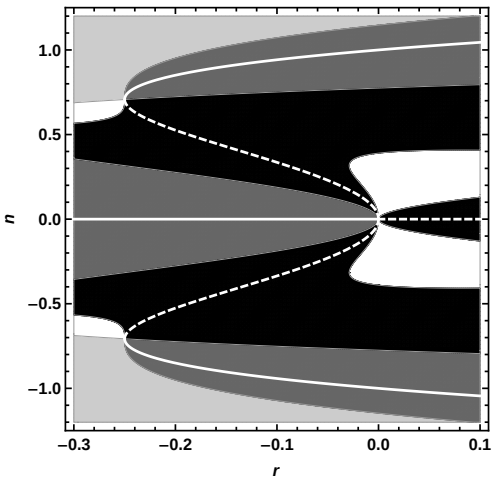

Fig. 6. Enlarged figure of the part around $r = 0.1$ in Fig. 5. Note that the aspect ratio of this figure is different from that in Fig. 5. The hysteresis jump from the equilibrium point to the other point goes through the non-equilibrium region. The one jump at $r = -0.25$, caused by the decrease in r, goes through a J-unstable region. The other jump at $r = 0$, caused by the increase in r, goes through J-unstable and J-stable regions.

hysteresis jumps in the subcritical pitchfork bifurcation differ qualitatively from each other from a KCC theory viewpoint.

The subcritical bifurcation is known to be related to discontinuous or first-order phase transitions. In the engineering literature, the subcritical bifurcation is hard or dangerous, because of the jump from zero to large amplitude [Strogatz, 2014]. The results described above show that this hard jump is expected to be accompanied by spiral-like behavior in the J-stable region.

6.3. *Dynamics of production process around equilibrium points*

We consider the dynamics of the production process around equilibrium points $n = 0$ and $n^*_{a\pm}, n^*_{b\pm}$ defined by (42), (43). First, we consider J-stability of the production process around the equilibrium points: i.e., node or spiral. From Eq. (48), we have

$$P(n) = \begin{cases} \frac{r^2}{4}, & n = 0, \\ -\frac{1}{2}(1+4r)(-1-2r+\sqrt{1+4r}), & n = n^*_{a\pm}, \\ \frac{1}{2}(1+4r)(1+2r+\sqrt{1+4r}), & n = n^*_{b\pm}. \end{cases} \tag{56}$$

Since $P \geq 0$, the equilibrium points of the system show node type (Fig.1).

Next, we consider the N-stability around the equilibrium points, i.e., the linear stability. From (46), we have

$$N(n) = \begin{cases} -\frac{r}{2}, & n = 0, \\ \frac{1}{2}(1+4r-\sqrt{1+4r}), & n = n^*_{a\pm}, \\ \frac{1}{2}(1+4r+\sqrt{1+4r}), & n = n^*_{b\pm}. \end{cases} \tag{57}$$

When $r < -1/4$, only $N(0)$ takes the a real value and is positive, so there is one stable point $n = 0$. When $-1/4 < r < 0$, the non-linear connections $N(0)$ and $N(n^*_{b\pm})$ are positive and $N(n^*_{a\pm})$ is negative, so there are three stable points $n = 0, n^*_{b\pm}$ and two unstable points $n = n^*_{a\pm}$. When $r > 0$, the non-linear connection $N(n^*_{a\pm})$ and $N(n^*_{b\pm})$ are positive and $N(0)$ is negative. However, the point $n = n^*_{a\pm}$ is not a real value for $r > 0$, so there are two stable points $n^*_{b\pm}$ and one unstable point: $n = 0$. That is, the production process also shows a subcritical pitchfork bifurcation.

7. Discussion

7.1. *Time dependence of stability*

In this paper, we derived the geometric quantities regarding the ODE with bifurcations, because KCC theory has shown that the geometric quantities, such as the non-linear connection N and the deviation curvature P, are related to the stability of the system. Generally, the stability does not depend on time around the equilibrium points. In fact, N and P around the equilibrium points are independent of time, such as in (24); (31); (38) and (39); (56) and (57).

In contrast, N in the non-equilibrium region does depend on time, such as (21), (28), (35), and (46). For pitchfork bifurcations, P in the non-equilibrium region also depends on time: (37) and (48). For saddle-node and transcritical bifurcations, P in the non-equilibrium region does not depend on time: (23) and (30).

In summary, the stability structure of pitchfork bifurcations depends on time in the non-equilibrium region. That is, the geometrical quantities of the pitchfork bifurcations, which control the stability of the original dynamic systems, (33) with (34), (44) with (45), themselves show another dynamic system in the non-equilibrium region, as in Eqs. (37) and (48). KCC theory implies that the stability structure of this other dynamic system can be described by other geometrical quantities, which will be mentioned in section 7.3.

7.2. *Higher-order term in subcritical pitchfork bifurcation*

In the analysis of the subcritical pitchfork bifurcation, we considered the higher order term n^5 in (40) to avoid the explosive instability. In this section, we consider the effect of the higher-order term from the viewpoint of KCC theory. For this, the system of the subcritical pitchfork bifurcation that does not have the higher-order term n^5 is analyzed:

$$\dot{n} = rn + n^3. \tag{58}$$

From $\dot{n} = 0$, we have $n^*_0 = 0$ and $n^*_\pm = \pm\sqrt{-r}$. When $r < 0$, there is one stable point, n^*_0, and two unstable points, $n^*_\pm$. When $r > 0$, there is one unstable point n^*_0. That is, Eq. (58) shows a subcritical pitchfork, just like Eq. (40).

By introducing the potential to (58), we can obtain the non-linear connection and the deviation curvature:

$$N = \frac{1}{2}(-r - 3a^2\dot{x}^2) = \frac{1}{2}(-r - 3n^2), \tag{59}$$

$$P = \frac{1}{4}\{r^2 - 6r(a\dot{x})^2 - 3(a\dot{x})^4)\} = \frac{1}{4}(r^2 - 6rn^2 - 3n^4). \tag{60}$$

From Eqs. (59) and (60), it can be found that there is no region in which the system is N-stable and J-stable. That is, the light gray region that can be seen in the higher-order case (Fig.5), does not exist in the lower-order case. This means that the non-equilibrium dynamics of the lower-order case differ from those of the higher-order case.

However, around the equilibrium points, we have

$$N = \begin{cases} -\frac{1}{2}r, & n = n_0^*, \\ r, & n = n_\pm^*. \end{cases} \tag{61}$$

From (61), the potential also shows the subcritical pitchfork, in agreement with the higher-order case. From the results described here, the effect of the higher-order term may be closely related to the geometric quantities in the non-equilibrium region. In the next section, we discuss this point using the Douglas tensor, which is one of the invariant quantities in KCC theory,

7.3. *Douglas tensor and higher-order term in one-dimensional bifurcation system*

In this section, we discuss the higher-order term of the bifurcation system from the viewpoint of the invariant quantities in KCC theory. This paper has considered the non-linear connection and the deviation curvature, which is one of the invariant quantities in KCC theory. According to previous papers, there are three other invariant quantities in KCC theory: the torsion tensor T^i_{jk}, the Riemann-Christoffel curvature tensor R^i_{jkl}, and the Douglas tensor D^i_{jkl} (e.g., [Douglas, 1927; Antonelli, & Bucataru, 2003]). These are defined as

$$T^i_{jk} = \frac{1}{3}\left(\frac{\partial P^i_j}{\partial \dot{x}^k} - \frac{\partial P^i_k}{\partial \dot{x}^j}\right), \tag{62}$$

$$R^i_{jkl} = \frac{\partial T^i_{jk}}{\partial \dot{x}^l}, \tag{63}$$

$$D^i_{jkl} = \frac{\partial G^i_{jk}}{\partial \dot{x}^l}, \tag{64}$$

where P^i_j is the deviation curvature, defined by (11), and G^i_{jk} is the Finsler connection, defined by (13). In previous analyses of KCC theory, the Douglas tensor has not received attention, because the function D^i_{jkl} often takes a zero value in an ordinary system. In a one-dimensional bifurcation system, however, the function D^i_{jkl} can take non-zero values, so we pay attention to it here. Other functions, such as T^i_{jk} and R^i_{jkl}, vanish from the definition in a one-dimensional system, so we do not consider them.

Let us derive the Douglas tensor in the bifurcation system used in this paper. In the saddle-node bifurcation and the transcritical bifurcation, the Finsler connection $G^1_{11} = G$ is a constant ((22) and (29)), so the Douglas tensor becomes zero. In the supercritical pitchfork bifurcation, Eq. (36): $G = 3a^2\dot{x}$ shows that the Douglas tensor is a constant:

$$D = \frac{\partial G}{\partial \dot{x}} = 3a^2, \tag{65}$$

where we set $D^1_{111} = D$.

In the subcritical pitchfork bifurcation, Eq. (47): $G = -3a^2\dot{x} + 10a^4\dot{x}^3$ shows that the Douglas tensor is not a constant:

$$D = 3a^2(10n^2 - 1). \tag{66}$$

Thus, the sign of the Douglas tenser depends on the value of $n = a\dot{x}$. However, in the system (58), the subcritical pitchfork bifurcation with a lower-order term, gives $D = -3a^2$, which differs from (66).

We consider the case in which the Douglas tensor gives a non-zero value from the viewpoint of the order of the term. The form of the basic equation considered in this paper is given by $\ddot{x} + g = 0$, where g shows the type of the bifurcation, such as (20) in a saddle-node bifurcation, $g = -r/a - a\dot{x}^2$ (27) in a transcritical bifurcation, $g = -r\dot{x} + a\dot{x}^2$, (34) in a supercritical pitchfork bifurcation, $g = -r\dot{x} + a^2\dot{x}^3$, and (45) in a subcritical pitchfork bifurcation, $g = -r\dot{x} - a^2\dot{x}^3 + a^4\dot{x}^5$. In one-dimensional space, the term g is related to the Douglas tensor through the following relationship:

$$D = \frac{1}{2}\frac{\partial^3 g}{\partial \dot{x}^3}, \tag{67}$$

where we use (64), (13): $G = \partial N/\partial\dot{x}$ and (12): $N = (1/2)\partial g/\partial\dot{x}$ in one-dimensional space. Thus, if g includes higher-order terms than $\dot{x}^2$, such as the pitchfork bifurcations, the Douglas tensor returns a non-zero value. From $n = a\dot{x}$, the case $D \neq 0$ means that the normal form of the bifurcation system includes higher-order terms than n^2, such as (32) in supercritical pitchforks, $\dot{n} = rn - n^3$, and (40) in subcritical pitchforks, $\dot{n} = rn + n^3 - n^5$. Thus, the Douglas tensor plays an important role in the analysis of the normal form when it includes higher-order terms than a second-order term.

Next, we consider how the Douglas tensor is related to N-stability and J-stability. From (12), (13), and (17) in one-dimensional space, we have

$$\frac{\partial^2 N}{\partial \dot{x}^2} = D, \tag{68}$$

$$\frac{\partial P}{\partial \dot{x}} = -gD. \tag{69}$$

Around the equilibrium points, both N and P, i.e., both N-stability and J-stability, are independent of $\dot{x}$, such as (56) and (57), so the Douglas tensor vanishes. That is, the Douglas tensor is related to the non-equilibrium behavior of the N-stability and J-stability. For example, as mentioned above, the stability structure of the pitchfork bifurcations depends on time in the non-equilibrium region. In this case, the Douglas tensor does not vanish but describes the non-equilibrium dynamics of the stability of the pitchfork bifurcation via the equation, such as (66). Moreover, it is found that the bifurcation parameter r is not included in Eq. (66), because r is related to the lower term of $\dot{x}$ in the normal form. This implies that the Douglas tensor can describe the dynamics beyond the bifurcation.

In the previous stability analysis, we have often considered a system that includes a lower-order term, and the stability analysis is made around the equilibrium points, so the Douglas tensor has not been noticed. As described above, however, the Douglas tensor is expected to be a useful invariant quantity to consider how the higher-order term in the bifurcation system affects N-stability and J-stability in the non-equilibrium region.

7.4. *Time-like potentials and ecological systems*

In this paper, we consider the concept of time-like potential defined by $n = a\dot{x}$, where a is a positive constant. In ecological systems, the variable n corresponds to the number of individuals of the population. The population n physically exists, while the time-like potential x itself is a purely mathematical construct. However, by definition, the time-like potential corresponds to the time integral of the population. Hence, it is useful for describing the transient behavior of the production process. In fact, when the logistic equation is expressed in terms of the time-like potential, it has been shown to hold for real growth data from several species ([Antonelli, 1985; Antonelli, & Bucataru, 2003]). As logistic growth is the most fundamentally important classical process in ecology ([Antonelli, & Bucataru, 2003; Begon *et al.*, 2006]), our approach is useful for ecological systems analysis.

The relationship between Lyapunov stability and KCC theory, including Jacobi stability, has been analyzed in previous papers (e.g., [Abolghasem, 2012]). Finally, we briefly discuss this problem from the perspective of a time-like potential. Let V be a Lyapunov candidate function of the ecological system in terms of the time-like potential: $V = V(x(t))$. Lyapunov stability is related to the time-derivative of V: $\dot{V} = (\partial V/\partial x)(dx/dt) = (\nabla V)(n/a)$. As n is positive in the ecological system and a is positive in this paper, the sign of $\dot{V}$ depends only on the gradient of V in the ecological system. Therefore, Lyapunov stability, such as stable equilibrium or globally asymptotically stable equilibrium, is related to the gradient of the function of the time-like potential. It will be interesting to develop these concepts in future work.

8. Conclusions

Our main conclusions are as follows.

(1) By introducing the concept of a time-like potential, we can apply the KCC theory to the typical example of one-dimensional bifurcations. This means that we can derive the geometric invariants of the bifurcations, and analyze the non-equilibrium dynamics of the ODE with bifurcations.
(2) For example, the non-equilibrium region, where the hysteresis jumps from one equilibrium point to the other, can be analyzed based on KCC theory. We considered two hysteresis jumps in the subcritical pitchfork bifurcation. The one jump, caused by the decrease in the bifurcation parameter, goes through only the J-unstable region. The other jump, caused by the increase in the bifurcation parameter, goes through not only a J-unstable region but also a J-stable region. That is, the two jumps differ qualitatively from each other from the viewpoint of KCC theory.
(3) In the non-equilibrium region, the deviation curvature in the saddle-node and the transcritical bifurcation is a function of only the bifurcation parameter r, so J-stability does not depend on time. However, the deviation curvature in the pitchfork bifurcation is a function of r and the field n, so J-stability does depend on time. In this case, the geometric pattern in the r-n diagram becomes complex, but the equilibrium line is always included in the J-unstable region. That is, a J-stable region can be observed in the non-equilibrium region.
(4) The Douglas tensor is one of the invariant quantities in KCC theory, and it has not received attention in previous stability analyses. This paper has shown that the Douglas tensor is useful to consider how the higher-order term in the bifurcation system affects N-stability and J-stability in the non-equilibrium region.

Acknowledgments

The authors would like to thank the anonymous referees for their helpful and valuable comments.

References

Abolghasem, H. [2012] "Liapunov stability versus Jacobi stability," *J. Dyn. Syst. Geom. Theor.* **10**, 13–32.
Antonelli, P.L. [1985] *Mathematical essays on growth and the emergence of form*, (University of Alberta Press, Alberta).

Antonelli, P.L., Ingarden, R.S. & Matsumoto, M. [1993] *The theory of sprays and Finsler spaces with applications in physics and biology*, (Kluwer, Dordrecht).

Antonelli, P.L. & Bucataru, I. [2001] "Volterra-Hamilton production models with discounting: general theory and worked examples," *Nonlinear Anal. RWA.* **2**, 337–356.

Antonelli, P.L., Rutz, S.F., & Sabău, S.V. [2002] "A transient-state analysis of Tyson 's model for the cell division cycle by means of KCC-theory," *Open Syst. Inf. Dyn.* **9**, 222–238.

Antonelli,, P.L. & Bucataru, I. [2003] *KCC theory of a system of second order differential equations, in: Handbook of Finsler Geometry*, (Kluwer, Academic Dordrecht).

Antonelli, P.L., Leandro, E.S., & Rutz, S.F. [2014] "Gradient-driven dynamics on Finsler manifolds: the Jacobi action-metric theorem and an application in ecology," *Nonlinear Stud.* **21**, 141–152.

Balan, V. & Neagu, M. [2010] "Jet geometrical extension of the KCC-invariants," *Balkan J. Geom. Appl.* **15**, 8–16.

Begon, M., Townsend, C.R. & Harper, J.L. [2006] *Ecology: From Individuals to Ecosystems*, (Blackwell Publishing, Malden, MA).

Boehmer, C.G. & Harko, T. [2010] "Nonlinear stability analysis of the emden-fowler equation," *J. Nonlinera. Math. Phy.* **17**, 503–516.

Borresen, J. & Lynch, S. [2002] "Further investigation of hysteresis in Chua's circuit," *Int. J. Bifurcat. Chaos* **12**, 129-134.

Bucataru, I., Constantinescu, O. & Dahl, M.F. [2011] "A geometric setting for systems of ordinary differential equations," *Int. J. Geo. Meth. Mod. Phy.* **8**, 1291–1327.

Burguete, J. & De La Torre, A. [2009] "Hysteresis and vortices dynamics in a turbulent flow," *Int. J. Bifurcat. Chaos* **19**, 2695-2703.

Douglas, J. [1927] "The general geometry of paths," *Ann. Math.* **29**, 143–168.

Dănilă, B., Harko, T., Mak, M.K., Pantaragphong, P. & Sabău, S.V. [2016] "Jacobi stability analysis of scalar field models with minimal coupling to gravity in a cosmological background," *Adv. High Ene. Phy.* **2016**, p. 26.

Gupta, M.K. & Yadav, C.K. [2016] "Jacobi stability analysis of Rikitake system," *Int. J. Geo. Meth. Mod. Phy.* **13**, 1650098.

Harko, T. & Sabău, S.V. [2008] "Jacobi stability of the vacuum in the static spherically symmetric brane world models," *Phys. Rev. D.* **77**, 104009.

Harko, T., Ho, C.Y., Leung, C.S. & Yip, S. [2015] "Jacobi stability analysis of the Lorenz system," *Int. J. Geo. Meth. Mod. Phy.* **12**, 1550081.

Harko, T., Pantaragphong, P., & Sabău, S.V. [2016] "Kosambi-Cartan-Chern (KCC) theory for higher-order dynamical systems," *Int. J. Geo. Meth. Mod. Phy.* **13**, 1650014.

Lake, M.J. & Harko, T. [2016] "Dynamical behavior and Jacobi stability analysis of wound strings," *Eur. Phys. J.* **76**, 1–26.

Neagu, M. [2013] "Multi-time Kosambi-Cartan-Chern invariants and applications," *BSG Proceedings.* **20**, 36–50.

Nicola, I.R. & Balan, V. [2004] "Jacobi stability for dynamical systems with applications to biology", *Proc. of the 3-rd International Colloquium " Mathematics in Engineering and Numerical Physics*, 1320–1329.

Ramos, J., Lynch, S., Jones, D. & Degens, H. [2017] "Hysteresis in Muscle," *Int. J. Bifurcat. Chaos* **27**, 1730003.

Sabău, S.V. [2005] "Some remarks on Jacobi stability," *Nonlinear Anal. TMA.* **63**, e143–e153.

Sabău, S.V. [2005] "Systems biology and deviation curvature tensor," *Nonlinear Anal. RWA.* **6**, 563–587.

Strogatz, S.H. [2014] *Nonlinear dynamics and chaos: with applications to physics, biology, chemistry, and engineering*, (Westview press, USA).

Udrişte, C. & Nicola, I.R. [2007] "Jacobi stability for geometric dynamics," *J. Dyn. Syst. Geom. Theor.* **5**, 85–95.

Udrişte, C. & Nicola, I.R. [2009] "Jacobi stability of linearized geometric dynamics," *J. Dyn. Syst. Geom. Theor.* **7**, 161–173.

Wiggins, S. [2003] *Introduction to applied nonlinear dynamical systems and chaos*, (Springer-Verlag, New

York).

Yajima, T. & Nagahama, H. [2007] "KCC-theory and geometry of the Rikitake system," *J. Phys. A.* **40**, 2755–2772.

Yajima, T. & Yamasaki, K. [2016] "Jacobi stability for dynamical systems of two-dimensional second-order differential equations and application to overhead crane system," *Int. J. Geo. Meth. Mod. Phy.* **13**, 1650045.

Yamasaki, K. & Yajima, T. [2013] "Lotka-Volterra system and KCC theory: Differential geometric structure of competitions and predations," *Nonlinear Anal. RWA.* **14**, 1845–1853.

Yamasaki, K. & Yajima, T. [2016] "Differential geometric structure of non-equilibrium dynamics in competition and predation: Finsler geometry and KCC theory," *J. Dyn. Syst. Geom. Theor.* **14**, 137–153.